Biological Trace Element Research (2019) 187:107–119
https://doi.org/10.1007/s12011-018-1344-8

Liver Proteome of Mice with Distinct Genetic Susceptibilities to Fluorosis Treated with Different Concentrations of F in the Drinking Water

Zohaib Nisar Khan[1] · Isabela Tomazini Sabino[1] · Carina Guimarães de Souza Melo[1] · Tatiana Martini[1] · Heloísa Aparecida Barbosa da Silva Pereira[1,2] · Marília Afonso Rabelo Buzalaf[1]

Received: 17 October 2017 / Accepted: 10 April 2018 / Published online: 29 April 2018

Abstract

Appropriate doses of fluoride (F) have therapeutic action against dental caries, but higher levels can cause disturbances in soft and mineralized tissues. Interestingly, the susceptibility to the toxic effects of F is genetically determined. This study evaluated the effects of F on the liver proteome of mice susceptible (A/J) or resistant (129P3/J) to the effects of F. Weanling male A/J ($n = 12$) and 129P3/J ($n = 12$) mice were housed in pairs and assigned to two groups given low-F food and drinking water containing 15 or 50 ppm F for 6 weeks. Liver proteome profiles were examined using nano-LC-ESI-MS/MS. Difference in expression among the groups was determined using the PLGS software. Treatment with the lower F concentration provoked more pronounced alterations in fold change in liver proteins in comparison to the treatment with the higher F concentration. Interestingly, most of the proteins with fold change upon treatment with 15 ppm F were increased in the A/J mice compared with their 129P3/J counterparts, suggesting an attempt of the former to fight the deleterious effects of F. However, upon treatment with 50 ppm F, most proteins with fold change were decreased in the A/J mice compared with their 129P3/J counterparts, especially proteins related to oxidative stress and protein folding, which might be related to the higher susceptibility of the A/J animals to the deleterious effects of F. Our findings add light into the mechanisms underlying genetic susceptibility to fluorosis.

Keywords Liver · Fluoride · Fluorosis · Proteomics · Genetic susceptibility

Introduction

Fluorine is not only a common element present in the earth crust, but it is also found in the form of fluoride (F) in the soils, rocks, and water throughout the world. Higher concentrations are found in the areas where there have been recent/past pyroclastic activities or geologic uplift. In addition, fluoride is broadly employed in many industrial processes nowadays. The major sources of systemic fluoride exposure are the diet (food and water) and dental products, especially toothpastes [1].

Mild doses of fluoride have therapeutic action against dental caries while elevated levels, through intake of water, toothpastes, and diets containing high F levels will increase the body burden. The therapeutic window is very narrow, and there has been a lot of discussion concerning the appropriate levels of F intake to provide the maximum benefit (caries prevention) with minimum risk to cause disbenefits [2].

Once absorbed by the gastric intestinal system, F is distributed to all soft and mineralized tissues via the bloodstream [3]. Despite the most common adverse effects of excessive F intake are seen in the mineralized tissues (teeth and bones; dental and skeletal fluorosis, respectively) [4, 5], several studies that report the negative effects of F in soft tissues, such as the testis [6, 7], thyroid gland [8, 9], spleen [10, 11], liver [12], kidney [13, 14], and brain [15, 16], have been published.

Interestingly, the susceptibility to the toxic effects of F appears to be genetically determined. There are reports in the literature of populations that tend to develop higher levels of dental fluorosis than it would be expected from their background exposure to F [17–19]. Moreover, it was reported that inbred mice strains have different susceptibilities to dental fluorosis. The A/J strain is

✉ Marília Afonso Rabelo Buzalaf
mbuzalaf@fob.usp.br

[1] Department of Biological Sciences, Bauru School of Dentistry, University of São Paulo, Al. Octávio Pinheiro Brisolla, 9-75, Bauru, São Paulo 17012-901, Brazil

[2] Department of Genetics and Evolution, Center of Biological Sciences and the Health, Federal University of São Carlos, Washington Luis, Km 235, São Carlos, São Paulo 13560-970, Brazil

susceptible, with rapid onset and more severe development of dental fluorosis, while the 129P3/J strain is resistant, developing minimal dental fluorosis even under high exposure to F [20]. Despite the 129P3/J mice are resistant to the development of dental fluorosis, they excrete less F in urine and have higher circulating levels of F [21], which is very intriguing. Moreover, A/J mice drink higher volume of water than 129P3/J mice [21], which might be explained by the higher expression of α-AASA dehydrogenase (alpha-amino adipic semialdehyde dehydrogenase) in the latter [14], since this protein is an effective osmoprotectant.

Since the liver is a central organ in the metabolism, the metabolic differences shown by these animals in F handling prompted us recently to investigate the differential pattern of protein expression in the liver of these mice. We observed that A/J mice had many proteins increased when compared with their 129P3/J counterparts, most of them related to energy flux and oxidative stress, which could be implicated in their higher susceptibility to the development of dental fluorosis [22]. Thus, it is of great interest to evaluate the effect of F in the pattern of protein expression in the liver of A/J mice in comparison with 129P3/J mice, which was the aim of the present study.

Experimental section

Animal and Sample Collection

Weanling mice from two different inbred strains, A/J and 129P3/J (3-week-old; $n = 12$ from each strain), were kept in pairs in metabolic cages with ad libitum access to low-F food (AIN76A, 0.95 mg/kg F; PMI Nutrition, Richmond, IN, USA) and water containing 15 or 50 ppm F (as NaF) for a period of 42 days ($n = 6$ for each strain and level of F exposure). During the course of treatment, the humidity and temperature in the climate-controlled room were 23 ± 1 °C and 40–80%, respectively.

The experimental protocols were approved by the Ethics Committee for Animal Experiments of Bauru Dental School, University of São Paulo (license no. 031/2013). At the end of the study, the mice were anesthetized with ketamine/xylazine and the livers were collected for the study. Samples to be used for proteomic analysis were stored at − 80 °C, while those designated for F analysis were stored at − 20 °C.

Fluoride Analysis in the Liver

Fluoride analysis data was obtained with the ion-sensitive electrode, after hexamethyldisiloxane-facilitated diffusion [23], as previously described [12].

Statistical Analysis

The software GraphPad Prism version 6.0 for Windows (GraphPad Software, Inc., La Jolla, USA) was used to analyze differences in liver F concentration. Data passed normality (Kolmogorov-Smirnov test) and homogeneity (Bartlett test) and were then analyzed by two-way ANOVA followed by Sidak's multiple comparison test. The significance level was set at 5%.

Sample Preparation for Proteomic Analysis

Samples were prepared for proteomic analysis as previously described [24]. Cryogenic mill (model 6770; Spex, Metuchen, NJ, EUA) was used for the homogenization of frozen tissue. In order to extract proteins, liver homogenate was incubated in lysis buffer containing 7 M urea, 2 M thiourea, 4% CHAPS, 1% IPG buffer (pH 3–10), and 40 mM dithiothreitol (DTT) for 1 h at 4 °C with infrequent shaking. Afterwards, the homogenate was centrifuged at 15,000 rpm for 30 min at 4 °C and the supernatant having soluble proteins was collected. For the precipitation of proteins, PlusOne 2D Cleanup (GE Healthcare, Uppsala, Sweden) kit was used as recommended by the manufacturer. The pellets thus obtained were resuspended in rehydration buffer (7 M urea, 2 M thiourea, 0.5% CHAPS, 0.5% IPG buffer (pH 3–10), 18 mM DTT, 0.002% bromophenol blue). Later on, a protein pool was constituted while having 25 μL of liver proteins from each animal of the same group that was centrifuged for clarification. To each pool, 50 mM ammonium bicarbonate (AMBIC) containing 3 M urea was added. Each sample was filtered twice in 3 kDa Amicon (Millipore, St. Charles, MO, USA). Bradford protein assay [25] was done in order to quantify the proteins present in the pooled samples. To each sample (50 μg of total protein for each pool in a volume of 50 μL), 10 μL of 50 mM AMBIC was added. In sequence, 25 μL of 0.2% RapiGest™ (Waters Co., Manchester, UK) was added and incubated at 80 °C for 15 min. Afterwards, 2.5 μL of 100 mM DTT was added and incubated at 60 °C for 30 min. 2.5 μL of 300 mM iodoacetamide (IAA) was added and incubated for 30 min at room temperature (in the dark). Then, 10 μL of trypsin (100 ng; Trypsin Gold Mass Spectrometry; Promega, Madison, USA) was added and digestion was allowed to occur for 14 h at 37 °C. After digestion, 10 μl of 5% TFA was added, and the sample was left in an incubation phase for 90 min at 37 °C. It was then centrifuged (14,000 rpm for 30 min). Finally, the supernatant was collected and 5 μL of ADH (1 pmol/μL) plus 85 μL of 3% ACN was added to it.

LC-MS/MS and Bioinformatics Analyses

The nanoAcquity UPLC-Xevo QTof MS system (Waters, Manchester, UK) was used for the separation and

identification of peptides, exactly as previously described [26]. In order to notify the differences in the expression among the respective groups, Protein Lynx Global Service (PLGS) software was used, where $p < 0.05$ and $1 - p > 0.95$, and thus showed the downregulation or upregulation of proteins, respectively (Table 1). Bioinformatics analysis was performed, as reported earlier [24, 26–28]. For the comparison of A/J vs. 129P3/J, UniProt protein ID accession numbers were mapped back to their associated encoding UniProt gene entries. Furthermore, Gene Ontology annotation of broad biological process was performed using Cluego v2.0.7 + Clupedia v1.0.8, a Cytoscape plug-in. UniProt IDs were uploaded from Table 1 and analyzed with default parameters, which specify an enrichment (right-sided hypergeometric test) correction method using the Bonferroni step down, analysis mode "Function" and load gene cluster list for *Mus musculus*, evidence codes "All," set networking specificity "medium" (GO levels 3 to 8), and kappa score threshold 0.03. The protein-protein interaction networking was downloaded from PSICQUIC, built-in Cytoscape version 3.0.2, and constructed as proposed by Millan [29]. Ultimately, a network was constructed, providing a global view of potentially relevant interacting partners of proteins whose abundances change.

Results

Liver Fluoride Analysis

Liver F concentrations were significantly different between the strains ($F = 12.68$, $p = .002$) and F concentrations in the drinking water ($F = 36.55$, $p < 0.0001$), without interaction between these criteria ($F = 1.79$, $p = 0.196$). A dose-response pattern was observed for liver F concentrations. However, when the strains were compared, only the 129P3/J mice treated with 50 ppm F in the drinking water had liver F concentrations significantly higher than their A/J counterparts (Fig. 1).

Functional Distribution of Identified Proteins

Figure 2 shows, for each comparison, the functional classification according to the biological process with the most significant term. For the 15 ppm F (Fig. 2a) and 50 ppm F (Fig. 2b) groups, the identified proteins were divided into 14 and 12 functional categories, respectively. For both groups, the category with the highest percentage of the number of genes was the carboxylic acid metabolic process (24 and 31% for 15 and 50 ppm F, respectively), followed by the cellular amino acid metabolic process (13 and 22% for 15 and 50 ppm F, respectively).

Liver Proteome Profile and Identification of Differentially Expressed Proteins

Tables 1 and 2 show the proteins with changes in expression when A/J mice are compared with their 129P3/J counterparts for the groups treated with 15 and 50 ppm F, respectively. The treatment with the lower F concentration (15 ppm) provoked more pronounced alterations in fold change in comparison to the treatment with the higher F concentration (50 ppm). Remarkably, all proteins with fold change upon treatment with 15 ppm F were increased in the A/J mice compared with their 129P3/J counterparts. Among them are delta-amino levulinic acid dehydratase (P10518) and 3-ketoacyl-CoA thiolase A, peroxisomal (Q921H8) that were increased 5.58- and 4.18-fold in the A/J mice, in comparison with the 129P3/J mice. In addition, most of the unique proteins were identified in the A/J mice. Treatment with 50 ppm F caused less fold change in comparison with the treatment with 15 ppm F, with some proteins increased and others decreased in the A/J mice in comparison to their 129P3/J counterparts.

Protein Interaction Networks

A network was created for each of the comparisons displayed above, employing all the interactions found in the search conducted using PSICQUIC. After the global network was created, nodes and edges were filtered using the specification for *Mus musculus* taxonomy (10090). The value of fold change and also the p value were added in new columns. The ActiveModules 1.8 plug-in to Cytoscape was used to make active modules connected to subnetworks within the molecular interaction network whose genes presented significantly coordinated changes in fold changes and p value, as shown in the original proteomic analysis. Figure 3a, b shows the subnetwork generated by VizMapper for each comparison. Regardless of the F concentration, most of the proteins with fold change presented interaction with disks large homolog 4 (Q62108) and calcium-activated potassium channel subunit alpha-1 (Q08460) when the two strains were compared.

When the animals were treated with 15 ppm F, 7 proteins with fold change between the two strains interacted with disks large homolog 4 (Q62108), while 14 proteins with fold change presented interaction with calcium-activated potassium channel subunit alpha-1 (Q08460). Moreover, 11 proteins were upregulated and 5 proteins were downregulated in A/J mice, while 5 proteins were present only in A/J mice and another 5 proteins were present only in 129P3/J mice (Fig. 3a).

Table 1 Proteins with expression significantly altered in the liver of A/J and 129P3/J mice treated with 15 ppm F

Access number[a]	Gene name	Protein name description	PLGS score	Fold change	
				A/J (15 ppm)	129P3/J (15 ppm)
P10518	Alad	Delta-aminolevulinic acid dehydratase	113.6	5.58	− 5.58
Q921H8	Acaa1a	3-Ketoacyl-CoA thiolase A, peroxisomal	88.9	4.18	− 4.18
P24549	Aldh1a1	Retinal dehydrogenase 1	141.7	2.80	− 2.80
Q64442	Sord	Sorbitol dehydrogenase	277.3	2.29	− 2.29
Q8R0Y6	Aldh1l1	Cytosolic 10-formyltetrahydrofolate dehydrogenase	67.5	2.27	− 2.27
P24270	Cat	Catalase	183.6	1.75	− 1.75
Q64374	Rgn	Regucalcin	47.7	1.63	− 1.63
P26443	Glud1	Glutamate dehydrogenase 1, mitochondrial	279.4	1.62	− 1.62
Q9QXF8	Gnmt	Glycine *N*-methyltransferase	287.8	1.62	− 1.62
P62806	Hist1h4a	Histone H4	50.0	1.60	− 1.60
P62737	Acta2	Actin, aortic smooth muscle	139.1	1.51	− 1.51
P16015	Ca3	Carbonic anhydrase 3	308.3	1.49	− 1.49
P08228	Sod1	Superoxide dismutase [Cu-Zn]	105.8	1.49	− 1.49
P11725	Otc	Ornithine carbamoyl transferase, mitochondrial	150.3	1.46	− 1.46
P68134	Acta1	Actin, alpha skeletal muscle	195.6	1.43	− 1.43
P68033	Actc1	Actin, alpha cardiac muscle 1	195.6	1.42	− 1.42
O35490	Bhmt	Betaine–homocysteine *S*-methyltransferase 1	494.2	1.39	− 1.39
P60710	Actb	Actin, cytoplasmic 1	310.5	1.38	− 1.38
P10649	Gstm1	Glutathione *S*-transferase Mu 1	44.2	1.38	− 1.38
P07724	Alb	Serum albumin	285.4	1.36	− 1.36
P63260	Actg1	Actin, cytoplasmic 2	310.5	1.31	− 1.31
P56480	Atp5b	ATP synthase subunit beta, mitochondrial	33.7	1.28	− 1.28
O70456	Sfn	14-3-3 protein sigma	126.3	+	−
P63101	Ywhaz	14-3-3 protein zeta/delta	93.1	+	−
P49429	Hpd	4-Hydroxyphenylpyruvate dioxygenase	189.9	+	−
Q9JII6	Akr1a1	Alcohol dehydrogenase [NADP(+)]	60.2	+	−
P00329	Adh1	Alcohol dehydrogenase 1	184.8	+	−
P00330	ADH1	Alcohol dehydrogenase 1	68.6	+	−
O35945	Aldh1a7	Aldehyde dehydrogenase, cytosolic 1	105.0	+	−
Q8K023	Akr1c18	Aldo-keto reductase family 1 member C18	76.8	+	−
Q91ZU0	Asb7	Ankyrin repeat and SOCS box protein 7	99.9	+	−
Q61176	Arg1	Arginase-1	252.3	+	−
Q91YI0	Asl	Argininosuccinate lyase	71.8	+	−
Q9CQQ7	Atp5f1	ATP synthase subunit b, mitochondrial	55.9	+	−
Q9DB20	Atp5o	ATP synthase subunit O, mitochondrial	68.4	+	−
P21550	Eno3	Beta-enolase	194.7	+	−
P50172	Hsd11b1	Corticosteroid 11-beta-dehydrogenase isozyme 1	97.3	+	−
Q60773	Cdkn2d	Cyclin-dependent kinase 4 inhibitor D	71.4	+	−
Q9D8U7	Dtwd1	DTW domain-containing protein 1	64.2	+	−
O88513	Gmnn	Geminin	72.8	+	−
P24472	Gsta4	Glutathione *S*-transferase A4	160.1	+	−
P62827	Ran	GTP-binding nuclear protein Ran	74.8	+	−
P68433	Hist1h3a	Histone H3.1	490.5	+	−
P84228	Hist1h3b	Histone H3.2	490.5	+	−
P84244	H3f3a	Histone H3.3	461.5	+	−
P02301	H3f3c	Histone H3.3C	461.5	+	−

Table 1 (continued)

Access number[a]	Gene name	Protein name description	PLGS score	Fold change	
				A/J (15 ppm)	129P3/J (15 ppm)
Q9CPU0	Glo1	Lactoylglutathione lyase	436.0	+	−
Q5S006	Lrrk2	Leucine-rich repeat serine/threonine-protein kinase 2	11.4	+	−
Q8BPT6	Immp2l	Mitochondrial inner membrane protease subunit 2	73.9	+	−
Q9DC69	Ndufa9	NADH dehydrogenase [ubiquinone] 1 alpha subcomplex subunit 9, mitochondrial	88.0	+	−
O08807	Prdx4	Peroxiredoxin-4	160.8	+	−
P99029	Prdx5	Peroxiredoxin-5, mitochondrial	70.0	+	−
Q6PDH0	Phldb1	Pleckstrin homology-like domain family B member 1	49.6	+	−
Q8CD94	Lin52	Protein lin-52 homolog	92.8	+	−
E9Q401	Ryr2	Ryanodine receptor 2	12.3	+	−
Q91X83	Mat1a	*S*-adenosylmethionine synthase isoform type 1	288.0	+	−
P42209	sept1	Septin-1	67.0	+	−
Q8BR65	Suds3	Sin3 histone deacetylase corepressor complex component SDS3	68.2	+	−
O55060	Tpmt	Thiopurine *S*-methyltransferase	63.5	+	−
P34914	Ephx2	Bifunctional epoxide hydrolase 2	170.6	−	+
Q8VCU1	Ces3b	Carboxylesterase 3B	84.7	−	+
Q0VEJ0	Cep76	Centrosomal protein of 76 kDa	96.0	−	+
Q80YP0	Cdk3	Cyclin-dependent kinase 3	77.3	−	+
Q80XN0	Bdh1	D-Beta-hydroxybutyrate dehydrogenase, mitochondrial	127.0	−	+
Q811D0	Dlg1	Disks large homolog 1	48.8	−	+
O54734	Ddost	Dolichyl-diphosphooligosaccharide–protein glycosyltransferase 48 kDa subunit	42.7	−	+
P16858	Gapdh	Glyceraldehyde 3-phosphate dehydrogenase	211.8	−	+
Q61696	Hspa1a	Heat shock 70 kDa protein 1A	75.2	−	+
P17879	Hspa1b	Heat shock 70 kDa protein 1B	75.2	−	+
P16627	Hspa1l	Heat shock 70 kDa protein 1-like	75.2	−	+
P01868	Ighg1	Ig gamma-1 chain C region secreted form	89.2	−	+
Q9QZ29	Igbp1b	Immunoglobulin-binding protein 1b	84.8	−	+
P06151	Ldha	L-lactate dehydrogenase A chain	158.5	−	+
P34884	Mif	Macrophage migration inhibitory factor	122.3	−	+
P14152	Mdh1	Malate dehydrogenase, cytoplasmic	189.8	−	+
P27773	Pdia3	Protein disulfide isomerase A3	57.9	−	+
Q9DB54	Fam216a	Protein FAM216A	116.4	−	+
Q05920	Pc	Pyruvate carboxylase, mitochondrial	113.3	−	+
P17563	Selenbp1	Selenium-binding protein 1	101.1	−	+
Q63836	Selenbp2	Selenium-binding protein 2	101.1	−	+
Q9R0P3	Esd	*S*-formylglutathione hydrolase	57.7	−	+

The identified proteins are organized according to highest to lowest fold change. Plus sign indicates the presence of the protein, while minus sign indicates the absence of the protein in the respective groups

[a] Identification is based on protein ID from the UniProt protein database (http://www.uniprot.org/)

For the animals treated with 50 ppm F, 9 proteins with fold change interacted with disks large homolog 4 (Q62108), while 16 proteins with fold change interacted with calcium-activated potassium channel subunit alpha-1 (Q08460). Moreover, 7 proteins were upregulated and 13 proteins were downregulated in A/J mice, while 5 proteins were present only in A/J mice and another 7 proteins were present only in 129P3/J mice (Fig. 3b).

Discussion

Despite there are many reports highlighting the toxic effects of excessive F ingestion in different organs [14, 30–33], information related to the liver, especially to proteomics, is limited to two studies conducted with rats [34, 35]. The liver is an important organ in the body, which secretes bile and

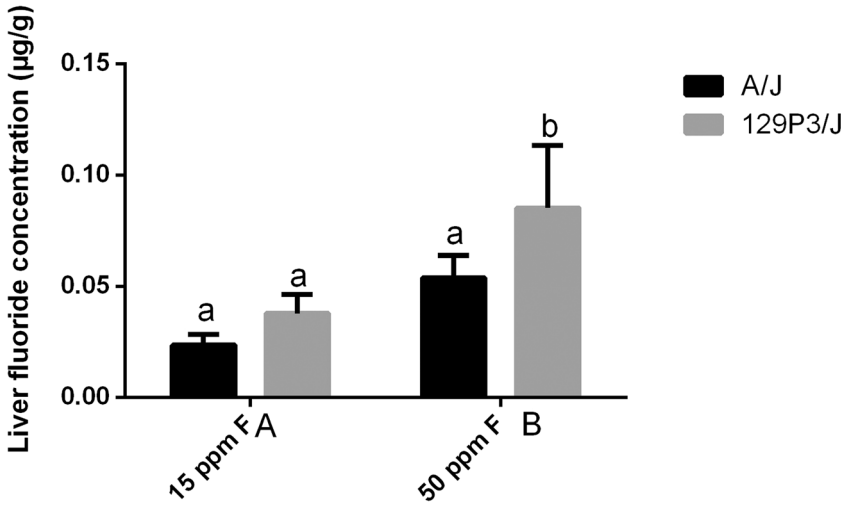

Fig. 1 Liver fluoride concentrations in the A/J and 129P3/J mice treated with water containing 15 or 50 ppm fluoride in the drinking water for 42 days. For each fluoride concentration, distinct lowercase letters indicate significant differences between the strains. Distinct uppercase letters denote significant differences between the fluoride concentrations. Two-way ANOVA and Sidak's test ($p < 0.05$). $n = 6$. Bars indicate SD

efficiently processes nutrients [36]. Moreover, the majority of toxicants are biotransformed into metabolites by the liver through various enzyme systems. Consequently, liver undergoes different levels of damage and alterations. These damage/alterations are often associated with a degenerative-necrotic condition [37]. Various reports have shown that drugs and other chemical substances can damage hepatocytes, thus leading to hepatic dysfunction [38–40]. In addition, excessive F intake can damage the liver and the degree of damage is related to the quantity of F ingested [41–43]. However, the mechanism of F-induced liver dysfunction remains unclear.

A/J and 129P3/J mice strains have been widely studied over the last few years because they respond quite differently to F exposure [14, 20, 44–46]. Thus, it is interesting to know if the distinct responses to F by these two strains are related to events occurring in the liver and what are the mechanisms involved. Recently, we observed that even without exposure to F, A/J mice had an increase in proteins related to energy flux and oxidative stress when compared to their 129P3/J counterparts [22], which seems to be a good explanation for the high susceptibility of these mice to the effects of F, since the exposure to this ion also induces oxidative stress [47–50]. Thus, it is of great interest to investigate the effects of both genetic background and F exposure on the liver proteomic profile, which was the main aim of the present study.

We observed a dose-response relationship in liver F concentrations, which confirms that the treatment with F was effective. Regarding the differences between the strains, despite 129P3/J mice had higher liver F concentrations when

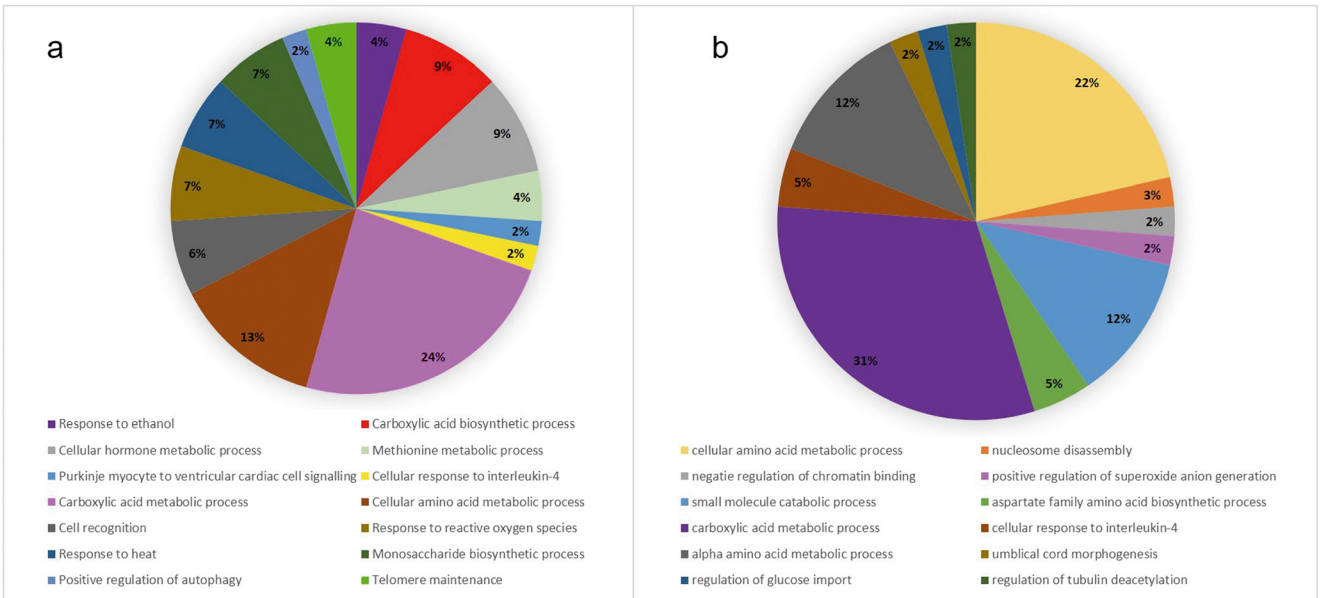

Fig. 2 Functional distribution of the proteins identified with differential expression in the liver of A/J compared to 129P3/J mice treated with fluoride (**a** 15 ppm and **b** 50 ppm). Categories of proteins were based on the GO annotation Biological Process. Significant terms (kappa = 0.03) and distribution were according to the percentage of the number of gene association

Table 2 Proteins with expression significantly altered in the liver of A/J and 129P3/J mice treated with 50 ppm F

Access number[a]	Gene name	Protein name description	PLGS score	Fold change	
				A/J (50 ppm)	129P3/J (50 ppm)
Q91VS7	Mgst1	Microsomal glutathione *S*-transferase 1	239.2	1.31	− 1.31
P11725	Otc	Ornithine carbamoyl transferase, mitochondrial	123.3	1.31	− 1.31
P26443	Glud1	Glutamate dehydrogenase 1, mitochondrial	269.9	1.28	− 1.28
P24549	Aldh1a1	Retinal dehydrogenase 1	385.7	1.28	− 1.28
P16015	Ca3	Carbonic anhydrase 3	340.1	1.25	− 1.25
P07724	Alb	Serum albumin	266.0	1.23	− 1.23
Q8C196	Cps1	Carbamoyl-phosphate synthase [ammonia], mitochondrial	1282.5	1.20	− 1.20
Q8VCU1	Ces3b	Carboxylesterase 3B	105.6	1.20	− 1.20
O35490	Bhmt	Betaine–homocysteine *S*-methyltransferase 1	561.6	1.18	− 1.18
Q9DCW4	Etfb	Electron transfer flavoprotein subunit beta	240.8	1.17	− 1.17
P54869	Hmgcs2	Hydroxymethylglutaryl-CoA synthase, mitochondrial	383.1	1.17	− 1.17
Q8BWT1	Acaa2	3-Ketoacyl-CoA thiolase, mitochondrial	1934.3	1.14	− 1.14
P02104	Hbb-y	Hemoglobin subunit epsilon-Y2	2492.3	1.06	− 1.06
P38647	Hspa9	Stress-70 protein, mitochondrial	115.4	− 0.55	0.55
P19157	Gstp1	Glutathione *S*-transferase P 1	4570.8	− 0.61	0.61
P46425	Gstp2	Glutathione *S*-transferase P 2	2746.8	− 0.61	0.61
P10853	Hist1h2bf	Histone H2B type 1-F/J/L	997.5	− 0.74	0.74
P10854	Hist1h2bm	Histone H2B type 1-M	997.5	− 0.74	0.74
Q6ZWY9	Hist1h2bc	Histone H2B type 1-C/E/G	997.5	− 0.75	0.75
Q8CGP2	Hist1h2bp	Histone H2B type 1-P	996.3	− 0.75	0.75
Q64525	Hist2h2bb	Histone H2B type 2-B	997.5	− 0.75	0.75
Q64524	Hist2h2be	Histone H2B type 2-E	964.4	− 0.75	0.75
Q9D2U9	Hist3h2ba	Histone H2B type 3-A	963.1	− 0.75	0.75
P02762	Mup6	Major urinary protein 6	1965.1	− 0.75	0.75
Q64475	Hist1h2bb	Histone H2B type 1-B	997.5	− 0.76	0.76
Q8CGP1	Hist1h2bk	Histone H2B type 1-K	997.5	− 0.76	0.76
Q8CGP0	Hist3h2bb	Histone H2B type 3-B	964.4	− 0.76	0.76
P11588	Mup1	Major urinary protein 1	1965.1	− 0.76	0.76
P11589	Mup2	Major urinary protein 2	1965.1	− 0.76	0.76
P04938	Mup8	Major urinary proteins 11 and 8 (fragment)	1965.1	− 0.76	0.76
Q64478	Hist1h2bh	Histone H2B type 1-H	997.5	− 0.77	0.77
B5X0G2	Mup17	Major urinary protein 17	1845.7	− 0.81	0.81
P52760	Hrsp12	Ribonuclease UK114	1703.5	− 0.84	0.84
P01942	Hba	Hemoglobin subunit alpha	6669.6	− 0.86	0.86
P56480	Atp5b	ATP synthase subunit beta, mitochondrial	1282.4	− 0.89	0.89
P10649	Gstm1	Glutathione *S*-transferase Mu 1	949.1	− 0.90	0.90
O35972	Mrpl23	39*S* ribosomal protein L23, mitochondrial	111.7	+	−
O08756	Hsd17b10	3-Hydroxyacyl-CoA dehydrogenase type 2	64.4	+	−
P14115	Rpl27a	60S ribosomal protein L27a	61.2	+	−
Q9CQJ0	Them5	Acyl-coenzyme A thioesterase THEM5	82.9	+	−
P17182	Eno1	Alpha-enolase	179.3	+	−
Q922J3	Clip1	CAP-Gly domain-containing linker protein 1	74.2	+	−
Q9D7F7	Chmp4c	Charged multivesicular body protein 4c	282.4	+	−
Q99LI2	Clcc1	Chloride channel CLIC-like protein 1	63.4	+	−
P50172	Hsd11b1	Corticosteroid 11-beta-dehydrogenase isozyme 1	99.7	+	−
Q60772	Cdkn2c	Cyclin-dependent kinase 4 inhibitor C	227.8	+	−

Table 2 (continued)

Access number[a]	Gene name	Protein name description	PLGS score	Fold change	
				A/J (50 ppm)	129P3/J (50 ppm)
P00405	Mtco2	Cytochrome c oxidase subunit 2	108.3	+	−
O35215	Ddt	D-Dopachrome decarboxylase OS = *Mus musculus* GN = Ddt PE = 1 SV = 3	200.8	+	−
P58252	Eef2	Elongation factor 2	66.3	+	−
Q91XD4	Ftcd	Formimidoyl transferase-cyclodeaminase	156.9	+	−
P05064	Aldoa	Fructose-bisphosphate aldolase A	88.4	+	−
P16858	Gapdh	Glyceraldehyde 3-phosphate dehydrogenase	104.7	+	−
Q9WV93	Hey1	Hairy/enhancer-of-split related with YRPW motif protein 1	81.6	+	−
P43276	Hist1h1b	Histone H1.5	58.4	+	−
Q64522	Hist2h2ab	Histone H2A type 2-B	411.1	+	−
P08730	Krt13	Keratin, type I cytoskeletal 13	64.6	+	−
Q9R0H5	Krt71	Keratin, type II cytoskeletal 71	63.3	+	−
Q8BGZ7	Krt75	Keratin, type II cytoskeletal 75	79.2	+	−
Q9CPU0	Glo1	Lactoylglutathione lyase	462.7	+	−
Q05CL8	Larp7	La-related protein 7	57.8	+	−
P41216	Acsl1	Long-chain-fatty-acid–CoA ligase 1	105.5	+	−
Q9D7Q0	Lyg1	Lysozyme g-like protein 1	70.8	+	−
Q9JLB0	Mpp6	MAGUK p55 subfamily member 6	66.5	+	−
Q99NA9	Pcgf6	Polycomb group RING finger protein 6	81.7	+	−
P27773	Pdia3	Protein disulfide isomerase A3	133.8	+	−
O55125	Nipsnap1	Protein NipSnap homolog 1	98.8	+	−
P61458	Pcbd1	Pterin-4-alpha-carbinolamine dehydratase	133.6	+	−
Q05920	Pc	Pyruvate carboxylase, mitochondrial	61.1	+	−
Q3THS6	Mat2a	*S*-Adenosylmethionine synthase isoform type 2	81.6	+	−
Q07417	Acads	Short-chain specific acyl-CoA dehydrogenase, mitochondrial	83.5	+	−
Q9D9R3	Spata9	Spermatogenesis-associated protein 9	120.2	+	−
Q8VE22	Mrps23	28*S* ribosomal protein S23, mitochondrial	96.5	−	+
Q78JT3	Haao	3-Hydroxyanthranilate 3,4-dioxygenase	172.7	−	+
P49429	Hpd	4-Hydroxyphenylpyruvate dioxygenase	129.3	−	+
P50247	Ahcy	Adenosylhomocysteinase	137.7	−	+
P00329	Adh1	Alcohol dehydrogenase 1	202.1	−	+
O35945	Aldh1a7	Aldehyde dehydrogenase, cytosolic 1	113.9	−	+
Q00623	Apoa1	Apolipoprotein A-I	95.3	−	+
P05201	Got1	Aspartate aminotransferase, cytoplasmic	110.3	−	+
Q8CHT0	Aldh4a1	Delta-1-pyrroline-5-carboxylate dehydrogenase, mitochondrial	93.9	−	+
P10518	Alad	Delta-aminolevulinic acid dehydratase	274.5	−	+
P19639	Gstm3	Glutathione *S*-transferase Mu 3	220.8	−	+
P07901	Hsp90aa1	Heat shock protein HSP 90-alpha	109.4	−	+
P11499	Hsp90ab1	Heat shock protein HSP 90-beta	226.1	−	+
P70696	Hist1h2ba	Histone H2B type 1-A	101.1	−	+
Q61425	Hadh	Hydroxyacyl-coenzyme A dehydrogenase, mitochondrial	86.2	−	+
P05784	Krt18	Keratin, type I cytoskeletal 18	137.8	−	+
P06151	Ldha	L-Lactate dehydrogenase A chain	168.9	−	+
Q9DAT2	Mrgbp	MRG/MORF4L-binding protein	163.6	−	+
Q80VA0	Galnt7	*N*-Acetylgalactosaminyltransferase 7	84.2	−	+
Q9CR61	Ndufb7	NADH dehydrogenase [ubiquinone] 1 beta subcomplex subunit 7	125.5	−	+
P17742	Ppia	Peptidyl-prolyl *cis-trans* isomerase A	258.1	−	+

Table 2 (continued)

Access number[a]	Gene name	Protein name description	PLGS score	Fold change	
				A/J (50 ppm)	129P3/J (50 ppm)
P70296	Pebp1	Phosphatidylethanolamine-binding protein 1	273.3	−	+
P58659	Eva1c	Protein eva-1 homolog C	92.8	−	+
O70622	Rtn2	Reticulon-2	109.8	−	+
B2RY56	Rbm25	RNA-binding protein 25	93.0	−	+
Q8BG73	Sh3bgrl2	SH3 domain-binding glutamic acid-rich-like protein 2	90.5	−	+
P59096	Stard6	StAR-related lipid transfer protein 6	135.8	−	+
Q8CHV6	Tada2a	Transcriptional adapter 2-alpha	85.2	−	+
Q8BMS1	Hadha	Trifunctional enzyme subunit alpha, mitochondrial	107	−	+
Q9CWR1	Wdr73	WD repeat-containing protein 73	93.7	−	+

The identified proteins are organized according to highest to lowest fold change. Plus sign indicates the presence of the protein, while minus sign indicates the absence of the protein in the respective groups

[a] Identification is based on protein ID from the UniProt protein database (http://www.uniprot.org/)

compared with their A/J counterparts, this difference was only significant for the highest F dose. This could be explained by the F uptake into the mineralized tissues, while higher doses of F could saturate the uptake [51]. The higher F concentrations found in the liver of 129P3/J mice is in-line with previous findings showing that these mice excrete less F and thus have higher circulating F levels than A/J mice, which is reflected in the F concentrations found in the bone, enamel, and different organs of these mice [44, 46, 52].

One remarkable finding of the present study was the fact that treatment with the lower F concentration (15 ppm) provoked more pronounced alterations in fold change in liver proteins in comparison to the treatment with the higher F concentration (50 ppm), which suggests low-dose hormesis of fluoride exposure. This is in-line with previous studies showing that treatment with 15 ppm F causes more alterations in the liver and kidney than treatment with 50 ppm F [34, 53, 54]. The reason for this finding is attributed to adaptive mechanisms of the organism to F [55] that are triggered by higher doses of this ion, but not by lower ones [54]. It is possible that if the treatment with 50 ppm F had been conducted for a shorter time, it could have led to more pronounced alterations, similar to the ones seen in the 15 ppm F group in the present study. In fact, F can have a dual effect (protective or toxic), depending on the dose and time of exposure [35, 53, 55–57]. Interestingly, all proteins with fold change upon treatment with 15 ppm F were increased in the A/J mice compared with their 129P3/J counterparts (Table 1), which suggests an attempt of the organism to fight the deleterious effects of F, since they seem to be dependent on the F dose and duration of the treatment [55]. Treatment with the lower F concentration also led to an increase in protein in the duodenum of rats after chronic exposure [58]. Among the increased proteins, the ones with the highest fold changes are related to metabolism (delta-aminolevulinic acid dehydratase (δ-ALA-D) and 3-ketoacyl-CoA thiolase A, peroxisomal with fold changes of 5.58 and 4.18, respectively. δ-ALA-D is a sulfhydryl-containing enzyme very sensitive to oxidizing agents [59]. It is essential in the heme biosynthesis [60], since it catalyzes the asymmetric condensation of two molecules of δ-ALA to porphobilinogen, which, in subsequent steps, is assembled into tetrapyrrole molecules that constitute the prosthetic groups of proteins and enzymes, such as catalase (CAT) [61]. CAT is an important antioxidant enzyme that is inhibited by F [62]. In fact, treatment with water containing 15 ppm F led to the lowest CAT activity in the liver of rats after treatment for 60 days [53], which is similar to the protocol employed in the present study. Thus, the increase in δ-ALA-D in our study might be an attempt to increase the activity of CAT, which is expected to be decreased upon treatment with F [53]. It is also important to highlight that in our previous study, where the animals were not treated with F, this enzyme was present only in the liver of A/J animals but not in their 129P3/J counterparts [22], which could be an attempt to fight against the oxidative stress in the first. Another protein, 3-ketoacyl-CoA thiolase A, peroxisomal, had an increase of 4.18 times in the A/J mice treated with 15 ppm F, in comparison to their 129P3/J counterparts. This protein is involved in the beta-oxidation of fatty acids, which is a multistep process by which fatty acids are broken down to produce energy. These events take place in mitochondria and peroxisomes, by mechanisms involving dehydrogenation, hydration, redehydrogenation, and thiolytic cleavage [63]. An increase in enzymes related to fatty acids beta-oxidation in the presence of F has been previously reported in the kidney [33, 64] and liver [34], suggesting a vigorous state of fatty acid metabolism, in attempt to counteract the inhibitory effect of F in the glycolytic pathway that has been known for a long time [65].

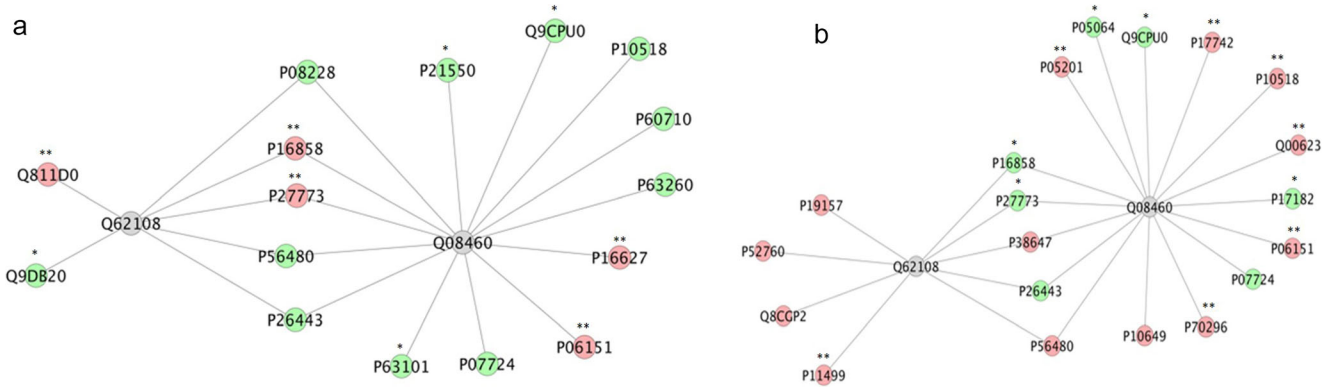

Fig. 3 **a** Subnetwork generated by VizMapper for the comparison of A/J vs. 129P3/J treated with 15 ppm fluoride. Color of node and single asterisk indicate the differential expression of the respective protein, for each comparison. Red and green nodes indicate protein downregulation and upregulation, respectively, while single asterisk and double asterisks indicate the presence and absence of protein, respectively, in the first group of each comparison. Gray node indicates proteins presenting interaction that were not identified in the present study. The access numbers in nodes correspond to the following: Q811D0 (Dlg1) disks large homolog 1; Q9DB20 (Atp5o) ATP synthase subunit O, mitochondrial; P08228 (Sod1) superoxide dismutase [Cu-Zn]; P16858 (Gapdh) glyceraldehyde 3-phosphate dehydrogenase; P27773 (Pdia3) protein disulfide isomerase A3; P56480 (Atp5b) ATP synthase subunit beta, mitochondrial; P26443 (Glud1) glutamate dehydrogenase 1, mitochondrial; P21550 (Eno3) beta-enolase; Q9CPU0 (Glo1) lactoylglutathione lyase; P10518 (Alad) delta-aminolevulinic acid dehydratase; P60710 (Actb) actin, cytoplasmic 1; P63260 (Actg1) actin, cytoplasmic 2; P16627 (Hspa1l) heat shock 70 kDa protein 1-like; P06151 (Ldha) L-lactate dehydrogenase A chain; P07724 (Alb) serum albumin; P63101 (Ywhaz) 14-3-3 protein zeta/delta; Q62108 (Dlg4) disks large homolog 4; Q08460 (Kcnma1) calcium-activated potassium channel subunit alpha-1. **b** Subnetwork generated by VizMapper for the comparison of A/J vs. 129P3/J treated with 50 ppm fluoride. Color of node and single asterisk indicate the differential expression of the respective protein, for each comparison. Red and green nodes indicate protein downregulation and upregulation, respectively, while single asterisk and double asterisks indicate the presence and absence of protein, respectively, in the first group of each comparison. Gray node indicates proteins presenting interaction that were not identified in the present study. The access numbers in nodes correspond to the following: Q8CGP2 (Hist1h2bp) histone H2B type 1-P; P11499 (Hsp90ab1) heat shock protein HSP 90-beta; P19157 (Gstp1) glutathione *S*-transferase P 1; P52760 (Hrsp12) ribonuclease UK114; P56480 (Atp5b) ATP synthase subunit beta, mitochondrial; P26443 (Glud1) glutamate dehydrogenase 1, mitochondrial; P38647 (Hspa9) stress-70 protein, mitochondrial; P27773 (Pdia3) protein disulfide isomerase A3; P16858 (Gapdh) glyceraldehyde 3-phosphate dehydrogenase; P10649 (Gstm1) glutathione *S*-transferase Mu 1; P05064 (Aldoa) fructose-bisphosphate aldolase A; P10518 (Alad) delta-aminolevulinic acid dehydratase; P06151 (Ldha) L-lactate dehydrogenase A chain; P70296 (Pebp1) phosphatidylethanolamine-binding protein 1; P05201 (Got1) aspartate aminotransferase, cytoplasmic; P17182 (Eno1) alpha-enolase; P17742 (Ppia) peptidyl-prolyl *cis-trans* isomerase A; Q00623 (Apoa1) apolipoprotein A-I; Q9CPU0 (Glo1) lactoylglutathione lyase; P07724 (Alb) serum albumin; Q08460 (Kcnma1) calcium-activated potassium channel subunit alpha-1; Q62108 (Dlg4) disks large homolog 4

On the other hand, different to what was seen for the animals treated with 15 ppm F, most of the proteins with fold change upon treatment with 50 ppm F were decreased in the A/J mice compared with their 129P3/J counterparts. The protein that presented the highest level of downregulation was *mitochondrial stress-70 protein*, that is a heat shock protein related to protein folding (UniProt). The downregulation means a lower degree of protein folding with consequently reduced toleration to F-induced stress in A/J mice [26, 34]. The other two proteins with the highest degree of downregulation in the A/J mice in the group treated with 50 ppm F were two isoforms of glutathione *S*-transferase (GST). GSTs are a multigene family of isozymes responsible for the detoxification of electrophiles by conjugation with the nucleophilic thiol-reduced GSH [66]. These enzymes play a crucial role in cellular detoxification of endogenous and xenobiotic substrates and in protection against oxidative stress [67]. Their downregulation means a difficulty of the A/J mice treated with 50 ppm F to fight oxidative stress. Despite most of the proteins with fold change in the A/J mice treated with 50 ppm F were downregulated in comparison with their 129P3/J counterparts, one of the upregulated proteins should be highlighted. This is the case of retinal dehydrogenase 1 (ALDH1A1). These enzymes are known to have an antioxidant role by producing NAD(P)H [68, 69], and the upregulation of ALDH1A1 might have been induced by the high dosage of F.

The two proteins in the center of the protein-protein interaction networks (calcium-activated potassium channel subunit alpha-1 and disks large homolog 4), regardless the F concentration, are related to potassium channels. Curiously, the same proteins were found in the center of the interaction networks in a previous study where A/J mice were compared with their 129P3/J counterparts without exposure to F [22]. This suggests that the pattern of the networks is driven mainly by the type of strain than by the exposure to F. In our previous study, the presence of these two interacting proteins in the center of the network was suggested to be related to alteration in the brain function of A/J mice [22] induced by accumulation of ammonia due to liver failure [70], but this needs to be investigated in further studies. Among the proteins identified with altered expression in the present study in the interaction networks, some of them were upregulated in the A/J mice,

regardless the F concentration in the drinking water. One of them was mitochondrial glutamate dehydrogenase 1 (GLUD1), a sensitive marker of hepatotoxicity. This enzyme is highly expressed in the hepatic mitochondria, and its upregulation supports the occurrence of mitochondrial dysfunction [71, 72], which is described to be induced upon exposure to F [34, 73]. Another upregulated protein in A/J mice, regardless exposure to F, was serum albumin. The main function of this protein is the regulation of the colloidal osmotic pressure of blood, since it has a good binding capacity for water, Ca^{2+}, Na^{+}, and K^{+} (UniProt). Its upregulation in A/J mice might be related to the higher volume of water ingested by this strain, regardless exposure to F [44].

In the network generated for the groups treated with 15 ppm F, most of the proteins with altered expression are associated with energy flux. The increase of the glycolytic enzyme beta-enolase, the reduction of L-lactate dehydrogenase, as well as the increase in subunits of ATP synthase involved in the oxidative phosphorylation indicate an increased energy flux in the A/J strain. This was also observed in our previous study that did not include exposure to F [22]. The increased energy flux might produce oxidative stress, which is reflected in the increased levels of SOD and ALAD.

Despite the network generated for the groups treated with 50 ppm F had the same proteins in the center as the one generated for the groups treated with 15 ppm F, some of the interacting partners were different. One of the downregulated proteins was histone H2B type 1-P. Despite not appearing in the network, many other isoforms of histones were downregulated in the A/J mice treated with 50 ppm F, as compared with their 129P3/J counterparts (Table 2). Histones are quite known as core components of nucleosome, and their reduction leads to disorganized and ineffectively structured genomic DNA, which might impair gene transcription [74]. This might help to explain the fact that most of the proteins with fold change upon treatment with 50 ppm F were decreased in the A/J mice compared with their 129P3/J counterparts.

In conclusion, treatment with the lower F concentration (15 ppm) provoked more pronounced alterations in fold change in liver proteins in comparison to the treatment with the higher F concentration (50 ppm), which is in-line with previous findings [34, 54, 75] and is possibly related to the duration of the treatment with F [55]. Interestingly, most of the proteins with fold change upon treatment with 15 ppm F were decreased in the A/J mice compared with their 129P3/J counterparts, suggesting an attempt of the latter to fight the deleterious effects of F. However, upon treatment with 50 ppm F, most proteins with fold change were decreased in the A/J mice compared with their 129P3/J counterparts, especially proteins related to oxidative stress and protein folding, which might be related to the higher susceptibility of the A/J animals to the deleterious effects of F. Our findings add light into the mechanisms underlying genetic susceptibility to fluorosis.

Acknowledgements The authors thank CNPq/TWAS for providing a scholarship to the first author (190145/2013-7).

References

1. Buzalaf MA, Levy SM (2011) Fluoride intake of children: considerations for dental caries and dental fluorosis. Monogr Oral Sci 22: 1–19
2. Rugg-Gunn AJ, Villa AE, Buzalaf MR (2011) Contemporary biological markers of exposure to fluoride. Monogr Oral Sci 22:37–51
3. Buzalaf MA, Whitford GM (2011) Fluoride metabolism. Monogr Oral Sci 22:20–36
4. Aoba T, Fejerskov O (2002) Dental fluorosis: chemistry and biology. Crit Rev Oral Biol Med 13:155–170
5. Krishnamachari KA (1986) Skeletal fluorosis in humans: a review of recent progress in the understanding of the disease. Prog Food Nutr Sci 10:279–314
6. Pushpalatha T, Srinivas M, Sreenivasula Reddy P (2005) Exposure to high fluoride concentration in drinking water will affect spermatogenesis and steroidogenesis in male albino rats. Biometals 18:207–212
7. Zhang S, Jiang C, Liu H, Guan Z, Zeng Q, Zhang C, Lei R, Xia T, Gao H, Yang L, Chen Y, Wu X, Zhang X, Cui Y, Yu L, Wang Z, Wang A (2013) Fluoride-elicited developmental testicular toxicity in rats: roles of endoplasmic reticulum stress and inflammatory response. Toxicol Appl Pharmacol 271:206–215
8. Ge YM, Ning HM, Wang SL, Wang JD (2005) DNA damage in thyroid gland cells of rats exposed to longterm intake of high fluoride and low iodine. Fluoride 38:318–323
9. Susheela AK, Bhatnagar M, Vig K, Mondal NK (2005) Excess fluoride ingestion and thyroid hormone derangements in children living in Delhi, India. Fluoride 38:98–108
10. Chen T, Cui HM, Cui Y, Bai CM, Gong T (2011) Decreased antioxidase activities and oxidative stress in the spleen of chickens fed on high-fluorine diets. Hum Exp Toxicol 30:1282–1286
11. Podder S, Chattopadhyay A, Bhattacharya S, Ray MR (2010) Histopathology and cell cycle alteration in the spleen of mice from low and high doses of sodium fluoride. Fluoride 43:237–245
12. Pereira HABD, Leite AD, Charone S, Lobo JGVM, Cestari TM, Peres-Buzalaf C et al (2013) Proteomic analysis of liver in rats chronically exposed to fluoride. PLoS One 8
13. Kobayashi CAN, Leite AL, Silva TL, Santos LD, Nogueira FCS, Oliveiraa RC et al (2009) Proteomic analysis of kidney in rats chronically exposed to fluoride. Chem Biol Interact 180:305–311
14. Carvalho JG, Leite AD, Peres-Buzalaf C, Salvato F, Labate CA, Everett ET et al (2013) Renal proteome in mice with different susceptibilities to fluorosis. PLoS One 8
15. Mullenix PJ, Denbesten PK, Schunior A, Kernan WJ (1995) Neurotoxicity of sodium-fluoride in rats. Neurotoxicol Teratol 17: 169–177
16. Niu RY, Zhang YL, Liu SL, Liu FY, Sun ZL, Wang JD (2015) Proteome alterations in cortex of mice exposed to fluoride and lead. Biol Trace Elem Res 164:99–105
17. Manji F, Baelum V, Fejerskov O (1986) Dental fluorosis in an area of Kenya with 2 ppm fluoride in the drinking-water. J Dent Res 65: 659–662
18. Manji F, Baelum V, Fejerskov O, Gemert W (1986) Enamel changes in 2 low-fluoride areas of Kenya. Caries Res 20:371–380
19. Yoder KM, Mabelya L, Robison VA, Dunipace AJ, Brizendine EJ, Stookey GK (1998) Severe dental fluorosis in a Tanzanian population consuming water with negligible fluoride concentration. Community Dent Oral Epidemiol 26:382–393

20. Everett ET, McHenry MAK, Reynolds N, Eggertsson H, Sullivan J, Kantmann C et al (2002) Dental fluorosis: variability among different inbred mouse strains. J Dent Res 81:794–798
21. Carvalho JG, Leite AL, Yan D, Everett ET, Whitford GM, Buzalaf MAR (2009) Influence of genetic background on fluoride metabolism in mice. J Dent Res 88:1054–1058
22. Khan ZN, Leite AL, Charone S, IT Sabino TM, Pereira HABS et al (2016) Liver proteome of mice with different genetic susceptibilities to the effects of fluoride. J Appl Oral Sci:250–257
23. Taves DR (1968) Separation of fluoride by rapid diffusion using hexamethyldisiloxane. Talanta 15:969–96&
24. Lobo JGVM, Leite AL, Pereira HABS, Fernandes MS, Peres-Buzalaf C, Sumida DH et al (2015) Low-level fluoride exposure increases insulin sensitivity in experimental diabetes. J Dent Res 94:990–997
25. Bradford MM (1976) A rapid and sensitive method for the quantitation of microgram quantities of protein utilizing the principle of protein-dye binding. Anal Biochem 72:248–254
26. Leite AL, Lobo JGVM, Pereira HABD, Fernandes MS, Martini T, Zucki F et al (2014) Proteomic analysis of gastrocnemius muscle in rats with streptozotocin-induced diabetes and chronically exposed to fluoride. PLoS One 9
27. Bauer-Mehren A (2013) Integration of genomic information with biological networks using Cytoscape. Methods Mol Biol 1021:37–61
28. Orchard S (2012) Molecular interaction databases. Proteomics 12: 1656–1662
29. Millan PP (2013) Visualization and analysis of biological networks. Methods Mol Biol 1021:63–88
30. Lima Leite A, Gualiume Vaz J, Lobo M, Barbosa HA, da Silva Pereira M, Silva Fernandes T, Martini FZ et al (2014) Proteomic analysis of gastrocnemius muscle in rats with streptozotocin-induced diabetes and chronically exposed to fluoride. PLoS One 9:e106646
31. Buzalaf MA, Caroselli EE, Cardoso de Oliveira R, Granjeiro JM, Whitford GM (2004) Nail and bone surface as biomarkers for acute fluoride exposure in rats. J Anal Toxicol 28:249–252
32. Buzalaf MA, Caroselli EE, de Carvalho JG, de Oliveira RC, da Silva Cardoso VE, Whitford GM (2005) Bone surface and whole bone as biomarkers for acute fluoride exposure. J Anal Toxicol 29: 810–813
33. Kobayashi CA, Leite AL, Silva TL, Santos LD, Nogueira FC, Oliveira RC et al (2009) Proteomic analysis of kidney in rats chronically exposed to fluoride. Chem Biol Interact 180:305–311
34. Pereira HA, Leite Ade L, Charone S, Lobo JG, Cestari TM, Peres-Buzalaf C et al (2013) Proteomic analysis of liver in rats chronically exposed to fluoride. PLoS One 8:e75343
35. Lobo JG, Leite AL, Pereira HA, Fernandes MS, Peres-Buzalaf C, Sumida DH et al (2015) Low-level fluoride exposure increases insulin sensitivity in experimental diabetes. J Dent Res 94(7):990
36. Zhou BH, Zhao J, Liu J, Zhang JL, Li J, Wang HW (2015) Fluoride-induced oxidative stress is involved in the morphological damage and dysfunction of liver in female mice. Chemosphere 139: 504–511
37. Mukhopadhyay D, Chattopadhyay A (2014) Induction of oxidative stress and related transcriptional effects of sodium fluoride in female zebrafish liver. Bull Environ Contam Toxicol 93:64–70
38. Sun K, Eriksson SE, Tan Y, Zhang L, Arner ES, Zhang J (2014) Serum thioredoxin reductase levels increase in response to chemically induced acute liver injury. Biochim Biophys Acta 1840:2105–2111
39. Wang X, Jiang Z, M Xing JF, Su Y, Sun L et al (2014) Interleukin-17 mediates triptolide-induced liver injury in mice. Food Chem Toxicol 71:33–41
40. Wang ZJ, Lee J, YX Si WW, Yang JM, Yin SJ et al (2014) A folding study of Antarctic krill (Euphausia superba) alkaline phosphatase using denaturants. Int J Biol Macromol 70:266–274
41. Xiong X, Liu J, He W, Xia T, He P, Chen X, Yang KD, Wang AG (2007) Dose-effect relationship between drinking water fluoride levels and damage to liver and kidney functions in children. Environ Res 103:112–116
42. Cao J, Chen J, Wang J, Jia R, Xue W, Luo Y, Gan X (2013) Effects of fluoride on liver apoptosis and Bcl-2, Bax protein expression in freshwater teleost, Cyprinus carpio. Chemosphere 91:1203–1212
43. Zlatkovic J, Todorovic N, Tomanovic N, Boskovic M, Djordjevic S, Lazarevic-Pasti T et al (2014) Chronic administration of fluoxetine or clozapine induces oxidative stress in rat liver: a histopathological study. Eur J Pharm Sci 59:20–30
44. Carvalho JG, Leite AL, Yan D, Everett ET, Whitford GM, Buzalaf MA (2009) Influence of genetic background on fluoride metabolism in mice. J Dent Res 88:1054–1058
45. Kobayashi CA, Leite AL, Peres-Buzalaf C, Carvalho JG, Whitford GM, Everett ET et al (2014) Bone response to fluoride exposure is influenced by genetics. PLoS One 9:e114343
46. Charone S, De Lima Leite A, Peres-Buzalaf C, Silva Fernandes M, Ferreira de Almeida L, Zardin Graeff MS et al (2016) Proteomics of secretory-stage and maturation-stage enamel of genetically distinct mice. Caries Res 50:24–31
47. Arguelles S, Garcia S, Maldonado M, Machado A, Ayala A (2004) Do the serum oxidative stress biomarkers provide a reasonable index of the general oxidative stress status? Biochim Biophys Acta 1674:251–259
48. Inkielewicz-Stepniak I, Czarnowski W (2010) Oxidative stress parameters in rats exposed to fluoride and caffeine. Food Chem Toxicol 48:1607–1611
49. Nabavia SM, Suredac A, Nabavia SF, Latifia AM, Moghaddam AH, Hellioe C (2012) Neuroprotective effects of silymarin on sodium fluoride-induced oxidative stress. J Fluor Chem 1425:79–82
50. Atmaca N, Atmaca HT, Kanici A, Anteplioglu T (2014) Protective effect of resveratrol on sodium fluoride-induced oxidative stress, hepatotoxicity and neurotoxicity in rats. Food Chem Toxicol 70: 191–197
51. Ekstrand J, Ericsson Y, Rosell S (1977) Absence of protein-bound fluoride from human and blood plasma. Arch Oral Biol 22:229–232
52. Everett ET, McHenry MA, Reynolds N, Eggertsson H, Sullivan J, Kantmann C et al (2002) Dental fluorosis: variability among different inbred mouse strains. J Dent Res 81:794–798
53. Iano FG, Ferreira MC, Quaggio GB, Mileni Silva Fernandes MS, Oliveira RC, Ximenes VF et al (2014) Effects of chronic fluoride intake on the antioxidant systems of the liver and kidney in rats. J Fluor Chem 168:212–217
54. Pereira HA, Dionizio AS, Fernandes MS, Araujo TT, Cestari TM, Buzalaf CP et al (2016) Fluoride intensifies hypercaloric diet-induced ER oxidative stress and alters lipid metabolism. PLoS One 11:e0158121
55. Dabrowska E, Letko R, Balunowska M (2006) Effect of sodium fluoride on the morphological picture of the rat liver exposed to NaF in drinking water. Adv Med Sci 51(Suppl 1):91–95
56. Barbier O, Arreola-Mendoza L, Del Razo LM (2010) Molecular mechanisms of fluoride toxicity. Chem Biol Interact 188:319–333
57. Dunipace AJ, Brizendine EJ, Zhang W, Wilson ME, Miller LL, Katz BP et al (1995) Effect of aging on animal response to chronic fluoride exposure. J Dent Res 74:358–368
58. Melo CGS, Perles J, Zanoni JN, Souza SRG, Santos EX, Leite AL et al (2017) Enteric innervation combined with proteomics for the evaluation of the effects of chronic fluoride exposure on the duodenum of rats. Sci Rep 7:1070
59. Bottari NB, Mendes RE, Baldissera MD, Bochi GV, Moresco RN, Leal ML et al (2016) Relation between iron metabolism and antioxidants enzymes and delta-ALA-D activity in rats experimentally infected by Fasciola hepatica. Exp Parasitol 165:58–63
60. Sassa S (1982) Delta-aminolevulinic acid dehydratase assay. Enzyme 28:133–145

61. Sassa S (1998) ALAD porphyria. Semin Liver Dis 18:95–101
62. Shanthakumari D, Srinivasalu S, Subramanian S (2004) Effect of fluoride intoxication on lipidperoxidation and antioxidant status in experimental rats. Toxicology 204:219–228
63. Wanders RJ, Waterham HR (2006) Biochemistry of mammalian peroxisomes revisited. Annu Rev Biochem 75:295–332
64. Xu H, Hu LS, Chang M, Jing L, Zhang XY, Li GS (2005) Proteomic analysis of kidney in fluoride-treated rat. Toxicol Lett 160:69–75
65. Warburg O, Chistian W (1941) Isohering und kristallisation des görungs ferments enolase. Biochem Zool 310:384–421
66. Hayes JD, Pulford DJ (1995) The glutathione S-transferase supergene family: regulation of GST and the contribution of the isoenzymes to cancer chemoprotection and drug resistance. Crit Rev Biochem Mol Biol 30:445–600
67. Schroer KT, Gibson AM, Sivaprasad U, Bass SA, Ericksen MB, Wills-Karp M et al (2011) Downregulation of glutathione S-transferase pi in asthma contributes to enhanced oxidative stress. J Allergy Clin Immunol 128:539–548
68. Pappa A, Chen C, Koutalos Y, Townsend AJ, Vasiliou V (2003) Aldh3a1 protects human corneal epithelial cells from ultraviolet- and 4-hydroxy-2-nonenal-induced oxidative damage. Free Radic Biol Med 34:1178–1189
69. Lassen N, Pappa A, Black WJ, Jester JV, Day BJ, Min E et al (2006) Antioxidant function of corneal ALDH3A1 in cultured stromal fibroblasts. Free Radic Biol Med 41:1459–1469
70. Felipo V (2013) Hepatic encephalopathy: effects of liver failure on brain function. Nat Rev Neurosci 14:851–858
71. Stanley CA (2009) Regulation of glutamate metabolism and insulin secretion by glutamate dehydrogenase in hypoglycemic children. Am J Clin Nutr 90:862S–866S
72. McGill MR, Sharpe MR, Williams CD, Taha M, Curry SC, Jaeschke H (2012) The mechanism underlying acetaminophen-induced hepatotoxicity in humans and mice involves mitochondrial damage and nuclear DNA fragmentation. J Clin Invest 122:1574–1583
73. Anuradha CD, Kanno S, Hirano S (2001) Oxidative damage to mitochondria is a preliminary step to caspase-3 activation in fluoride-induced apoptosis in HL-60 cells. Free Radic Biol Med 31:367–373
74. Chen R, Kang R, Fan XG, Tang D (2014) Release and activity of histone in diseases. Cell Death Dis 5:e1370
75. Jakubowski H (2006) Pathophysiological consequences of homocysteine excess. J Nutr 136:1741S–1749S